Capillary Aging of the Contacts between Glass Spheres and a Quartz Resonator Surface

J. N. D'Amour,[1] J. J. R. Stålgren,[1] K. K. Kanazawa,[1] C. W. Frank,[1,*] M. Rodahl,[2] and D. Johannsmann[3,†]

[1]*Department of Chemical Engineering, Stanford University, Stanford, California, 94305, USA*

[2]*Q-Sense AB, SE-426 77 Västra Frölunda, Sweden*

[3]*Institute of Physical Chemistry, Clausthal University of Technology, Arnold-Sommerfeld-Strasse 4, D-38678 Clausthal-Zellerfeld, Germany*

(Received 29 September 2005; published 7 February 2006)

The strength of the contacts between small glass spheres and the surface of a quartz crystal resonator has been probed based on the increase of resonance frequency induced upon sphere contact. The acoustic interaction between the sphere and the plate is modeled as a low-frequency coupled resonance; the dependence of the resonant parameters on overtone order lends support to this model. After exposing the sample to humid air and drying it again, the contact strength increases at least tenfold due to capillary forces—we observe a hysteretic form of the sand-castle effect. Repeated wet-dry cycles reveal logarithmic capillary aging with time. The experiments suggest that the drying of the liquid bridges leads to a contraction of small voids in the contact zone, subsequently increasing cohesion.

DOI: 10.1103/PhysRevLett.96.058301 PACS numbers: 83.80.Fg, 83.85.Vb, 77.65.Fs, 81.07.Lk

Wet granular materials are of tremendous importance in everyday life. The understanding of their static and dynamic behavior has implications in many diverse fields such as the pharmaceutical, construction, and agricultural industries as well as in a number of geophysical problems. The introduction of small amounts of liquid can dramatically alter the physical properties of granular assemblies [1,2]. This is commonly known as the sandcastle effect [3,4]. Underlying this phenomenon, interstitial liquid bridges form between particles through capillary action resulting in increased interparticle cohesion [5–8] and modified sliding friction [9–11]. Several studies have focused on interparticle forces of either granular assemblies or individual particles as a function of humidity or liquid content [4,5,12,13], aging time [5,13], resting angle [13], particle size [4,13], and solvent chemistry [12,13]. Quantifying the interparticle interactions is an important step in understanding the bulk mechanics of granular media.

The quartz crystal microbalance (QCM) is a well-known tool to probe the properties of materials on its surface based on acoustic interactions. As has first been pointed out by Dybwad, the QCM can be used to probe the elastic stiffness of a contact between the crystal surface and a sphere placed on the crystal [14]. The fact that the sphere *increases* the frequency (rather than decreasing it in proportion to its mass) points to a type of interaction where the increase in stiffness of the sphere-plate composite resonator outweighs the increase in mass. As such, this technique provides a new access to the mechanics of particle-plate contacts. Moreover, if the interaction between the crystal surface and the particle mimics the interparticle interaction—which is a reasonable assumption if the surface chemistry and the surface roughness are comparable—then the QCM can also probe the interparticle forces present in granular assemblies. Importantly, the technique is nondestructive [15]. Time-dependent phenomena like curing of an adhesive contact, sintering, capillary aging, or weakening of an adhesive bond under solvent exposure can be followed *in situ* without ever breaking a bond. Competing techniques usually quantify the adhesion via the force of detachment [16].

The experiments were performed with three different instruments. The first one was the QCM-D (Q-Sense), which probes frequency and dissipation based on the ring-down technique in the time domain. We also used a network analyzer (HP E5100, Hewlett-Packard) to measure the admittance spectrum including higher overtones (up to 75 MHz) and extracted frequency and bandwidth by curve fitting with the resonance curve. Finally, we used the RQCM (Maxtek), which measures frequency and resistance changes by means of a phase-locked-loop oscillator circuit.

Quartz crystals (Q-Sense) with a gold coating had a fundamental resonant frequency of 4.95 MHz and an rms surface roughness of less than 2 nm as measured by atomic force microscopy. Prior to measurement, the crystals were rinsed with pure ethanol, dried with nitrogen, and exposed to an oxygen plasma (75 W) for 5 min to remove organic residues, resulting in a hydrophilic surface. Borosilicate glass spheres (MO-SCI) with diameters D_S of 700 ± 50, 200 ± 20, 100 ± 20, and 45 ± 5 μm having an approximate surface roughnesses of 10–20 nm were used as received. The spheres were deposited by hand in an amount corresponding to a monolayer. Upon gentle tapping, they formed hexagonal arrays with a number density N [see Eq. (3)] equal to $2/3^{1/2}D_s^{-2}$. Temperature and humidity were controlled by means of a flow cell, where the humidity was regulated with two mass flow controllers in conjunction with a water channel.

Figure 1 shows the shifts in frequency and half band half width (Γ) obtained with 200 μm spheres in a typical sequence of wet-dry cycles taken with the QCM-D. When the spheres were first put down on the surface, the

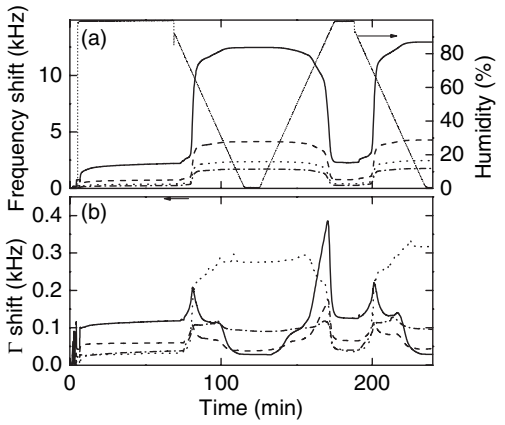

FIG. 1. Typical data set obtained while cycling between vapor and dry states for 200 μm spheres on a gold-coated quartz crystal. The solid, dashed, dotted, and dash-dotted lines represent the harmonics, 5 MHz, 15 MHz, 25 MHz, and 35 MHz, respectively. (a) The frequency peaks represent the dry states. The general procedure was to collect a baseline of the bare crystal, add the glass spheres (spheres were directly poured from the original vials onto the quartz crystal until monolayer coverage was realized—additional spheres above the monolayer had a negligible effect on resonant frequency though we minimized this in order to achieve mass transport uniformity of vapor between runs) and let stabilize, flow approximately 95% water vapor (the cell was kept at a slighter higher temperature, $\sim 1\,^{\circ}\mathrm{C}$, than the vapor channel to prevent droplet condensation) for an extended period of time (60–240 min), and then cycle between dry nitrogen and vapor states at select ramp rates and hold times. The fine dotted line represents the percent humidity. (b) The half band half width (Γ) trace shows peaks at the transitions between the wet and dry states. The conversion of dissipation ($D = Q^{-1}$) to Γ is $\Gamma = Df/2$.

frequency slightly increased at all resonances. Once the vapor was introduced, all harmonics experienced a further slow increase in frequency with time. After extended exposure to vapor, the cell atmosphere was ramped to the dry state. At approximately 65% relative humidity, the frequencies increased drastically along with a corresponding peak in bandwidth. The behavior of the crystal in subsequent wet-dry cycles was essentially reversible. All three instruments measured comparable increases in frequency and dissipative losses.

In the following, we describe how the strength of the sphere-plate contacts can be inferred from the (*positive*) frequency shift induced by a monolayer of rigid spheres [14]. Even though the distribution of forces presumably is complex, the essence of the model can be captured by representing the sphere by a point mass, m_s, coupled to the crystal through a complex spring with constant, $\tilde{\kappa} = \kappa + i\omega\xi$ where the real part, κ, represents an elastic force and the drag coefficient, ξ, quantifies a withdrawal of energy from the oscillation. The equation of motion for the mass-spring assembly is

$$m_s \frac{d^2 w}{dt^2} = -\kappa(w-u) - \xi \frac{d}{dt}(w-u), \qquad (1)$$

where $w = W\exp(i\omega t)$ and $u = U\exp(i\omega t)$ are the displacements of the sphere and the crystal surface, respectively. We define the resonant frequency and the damping coefficient of a sphere as $\omega_s = (\kappa/m_s)^{1/2}$ and $\gamma = \xi/m_s$, respectively. The sphere exerts a stress on the crystal proportional to the relative displacement, $w - u$, and the shear stiffness of the contact. The exerted stress, σ, is

$$\begin{aligned}\sigma &= -N(\kappa + i\omega\xi)(W-U) \\ &= Nm_s(\omega_s^2 + i\omega\gamma)\frac{\omega^2}{(\omega^2 - \omega_s^2 - i\omega\gamma)}U, \end{aligned} \qquad (2)$$

where N is the number of spheres per unit area (hexagonal packing in our case). The load impedance, Z_L, the ratio of stress to velocity, is given by

$$Z_L = \frac{\sigma}{i\omega U} = -iNm_s\omega\frac{(\omega_s^2 + i\omega\gamma)}{(\omega^2 - \omega_s^2 - i\omega\gamma)}. \qquad (3)$$

According to the small-load approximation [17], the complex frequency shift $\Delta\tilde{f} = \Delta f + i\Delta\Gamma$ is given by

$$\frac{\Delta f + i\Delta\Gamma}{f_f} = \frac{i}{\pi Z_q}Z_L = \frac{Nm_s\omega}{\pi Z_q}\frac{(\omega_s^2 + i\omega\gamma)}{(\omega^2 - \omega_s^2 - i\omega\gamma)}, \qquad (4)$$

where f_f is the frequency of the fundamental, Γ is the half band half width of the resonance, and $Z_q = 8.8 \times 10^6\ \mathrm{kg\,m^{-2}\,s^{-1}}$ is the acoustic impedance of AT-cut quartz. Equation (4) can also be derived from a continuum picture, modeling the contact regions and the spheres as a soft and a hard layer situated above each other. Using Eq. 18 in Ref. [18] and expanding all tangents to first order leads to an equation of the same form as Eq. (4).

At frequencies ω much less than ω_s, the motion of the sphere is in phase with the motion of the crystal. We obtain $\Delta f/f_f \approx -N\omega m_s/(\pi Z_q)$, which is equivalent to the Sauerbrey relation. In the opposing limit of $\omega \gg \omega_s$, a much different picture is found; one obtains [14,19–22]

$$\begin{aligned}\frac{\Delta f + i\Delta\Gamma}{f_f} &\approx \frac{Nm_s}{\pi Z_q\omega}(\omega_s^2 + i\omega\gamma) = \frac{N}{\pi Z_q\omega}(\kappa + i\omega\xi) \\ &\approx \frac{N}{2\pi^2 Z_q n f_f}(\kappa + i\omega\xi). \end{aligned} \qquad (5)$$

For $\omega \gg \omega_s$, inertia holds the spheres in place in the laboratory frame; only the stiffness of the contact is probed. The shifts of frequency and half band half width are proportional to κ and ξ, respectively. Our analysis rests on this simple relation. We have confirmed Eq. (5) by means of a rigorous electromechanical model that uses the mechanical impedance in Eq. (3) as a boundary condition [23]. Equation (5) predicts a positive frequency shift proportional to the inverse overtone order. As shown in Fig. 2, Δf scales as $1/n$, indicating that the condition $\omega \gg \omega_s$ underlying Eq. (5) is fulfilled. The scaling with $1/n$ is fulfilled a little less well for the smallest sphere size than for the other spheres. Calculating ω_S from the spring constant as determined with Eq. (5) and the mass of the spheres, one finds that ω_S is, indeed, comparable to ω for

these small spheres. A diameter around 40 μm is at the lower size limit of spheres that can be investigated with the technique described here.

Based on Eq. (5), we conclude that the strong increase in frequency observed after one wet-dry cycle should be attributed to an increased stiffness of the crystal-sphere contact. An increased cohesion after exposure to a liquid is known from dry sandcastles. Figure 2 also shows that the frequency shift increases with decreasing sphere size, which is a consequence of the increased packing density.

The interpretation of the wet-dry hysteresis is based on capillary forces arising from vapor condensing around the contacts [24,25]. The dependence of capillary forces on humidity, contact angle, surface roughness, mechanical compliance of the load-bearing asperities, shear stress, and time is an active field of research [11,13]. Wetting of the space between rough surfaces is known to be a hysteretic process in the sense that liquid bridges—once formed—persist after the vapor pressure is lowered again [5]. Figure 3 depicts a sketch (not to scale) of what we believe to occur. In the initial dry state, the contact is made across a few small asperities. These nanosized points of contact transport little stress and, therefore, are of almost no influence on the resonance properties. As the humidity increases, ring menisci form around the points of contact, which gradually increase the normal force and, as a consequence, the shear stiffness. When the Kelvin radius exceeds the scale of surface roughness, new liquid bridges form between asperities that were not initially in contact and liquid begins to fill large portions of the interparticle space. Also an elastic instability may occur, by which the wetted area around an asperity discontinuously increases, pulling the two surfaces together at the same time.

Upon drying, the radii of curvature of all menisci decrease. As a consequence, the Laplace pressure at the tip asperities increases and elastically deforms these regions into having greater contact. The ensuing solid-solid contacts are much stronger than the initial contacts as evidenced by the very substantial frequency increase. This strengthening is achieved by a convolution of an increased stiffness of the individual contacts and an increased number of contacts. This phenomenon differs from the sandcastle effect previously described [3,4] in that our granular medium displays increased stiffness *after it has dried.* We observe a hysteretic form of the sandcastle effect. An estimation of the forces involved shows that this scenario requires either nanoscale roughness or a mechanical stiffness of the load-bearing asperities, which is below the bulk modulus. Both seem possible.

In principle, the increased contact stiffness could also be caused by bridges of salt or contaminants accumulating at the points of contact. In order to check for the salt-bridge hypothesis, we used organic solvents, in which ionic compounds would be insoluble, and still observed wet-dry hysteresis, albeit with a smaller amplitude. To address the possible migration of surface contamination to the points of contact, we coated the gold electrode with a self-assembled monolayer (SAM) of 1-hexadecanethiol, which is hydrophobic. No wet-dry hysteresis was seen on the hydrophobic surface even though it should still attract contamination. However, upon subsequent oxygen plasma exposure to remove the SAM, hysteresis was once again observed.

The hypothesis that a deformation mechanism (asperity flattening or void contraction) underlies this hysteresis effect is corroborated by the maximum in half band half width, Γ, observed during the dry-wet and wet-dry transitions. The time at which this maximum occurs is different for the different overtones. This suggests that the peak in Γ relates to a shift in a retardation time, which passes through the accessible frequency window as the sample dries or fills with liquid. The deforming structure can be represented by a Voigt element—a dashpot with a drag coefficient, ξ_{loc}, in parallel with a spring with constant, κ_{loc}. This drag coefficient describes the dissipative interaction across the liquid; it should be inversely proportional to the height of the gap. The Voigt element gives rise to a retardation time of the order of $\xi_{\mathrm{loc}}/\kappa_{\mathrm{loc}}$, which shifts as the region around the asperity contracts or expands. The dissipation of the crystals peaks when the resonance frequency matches the inverse retardation time.

By repeatedly ramping the sample between dry and wet states over extended times, we proved the QCM to be a monitoring device of capillary aging. Bocquet *et al.* have

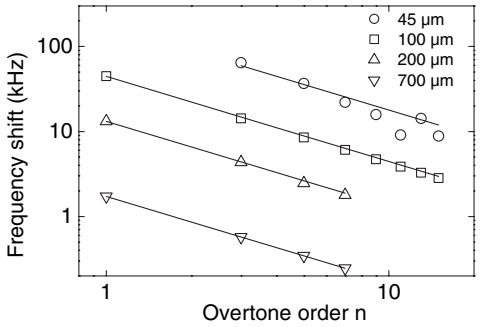

FIG. 2. Plot of the dry-state frequency shift vs overtone order. Straight lines for each sphere size have slope $1/n$ showing the inverse overtone dependence predicted by Eq. (5).

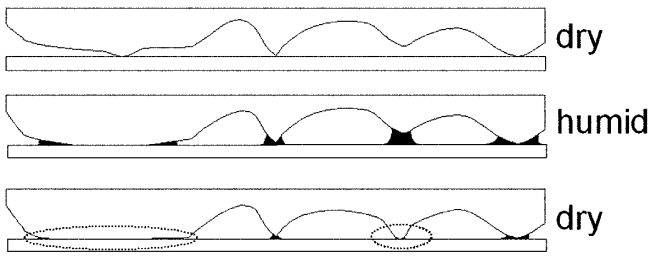

FIG. 3. Schematic drawing of the contact zone between the glass sphere and quartz resonator surface. The strength of the interparticle contact increases by either the formation of new bridges or by an elastic instability driven by the spreading of the wet area in a shallow wedge.

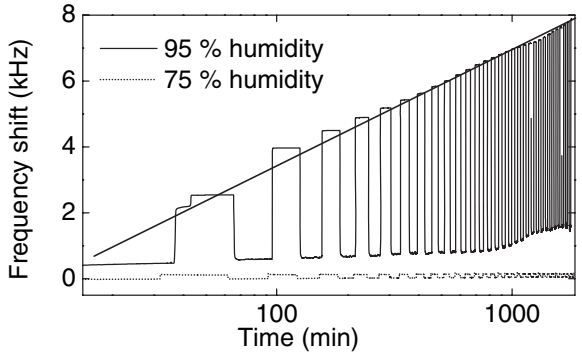

FIG. 4. Dry-state frequency shifts for 200 μm spheres at 95% and 75% humidity. Cycles between humid and dry states with step-change transitions lasted 60 min per cycle. The straight line drawn along the peaks of the 95% data trace illustrates logarithmic time dependence.

studied capillary aging based on the angle of first avalanche in a rotating drum [5]. This study probed aging in the wet state by disrupting the bonds, while we intermittently cycled the sample to the dry state and measured the shear stiffness of the contacts in this state. Given these differences, it is not obvious that the spring constant should increase logarithmically with time in the same way as the critical angle increased logarithmically in the experiments by Bocquet *et al.* Figure 4 shows changes in resonant frequency for experiments where the humidity was repeatedly cycled (30:30 min, wet:dry) between either 0% and 95% or 0% and 75%. The straight line represents a logarithmic aging. The fact that we find a logarithmic aging suggests that the shear stiffness is, indeed, a faithful indicator of interparticle cohesion.

Bocquet *et al.* argue that thermally activated formation of new liquid bridges—as opposed to asperity creep—is the mechanism underlying the aging kinetics [5]. We have tested these hypotheses by varying the cycle time. Since cycling produces local contractions of asperity regions, it should accelerate asperity creep, and one would expect the frequency shift for a given, fixed wet-state time to increase with the number of cycles. However, this is not the case, proving that creep is not the main aging mechanism. Only at the very late stage of the aging experiment (Fig. 4) do we observe some irreversibility in the sense that the wet state shows an increase in frequency with time. Simultaneously, the frequency shift in the dry state starts to deviate slightly from the logarithmic time dependence. Possibly, some creep sets in at this time.

In summary, probing the strength of particle-surface interactions via the frequency shift of a quartz crystal resonator gives insight into the details of the contact mechanics without disrupting bonds. A strong wet-dry hysteresis is observed, which is attributed to a hysteretic form of the sandcastle effect. In accordance with previous experiments using destructive techniques, we find logarithmic capillary aging, which indicates that the shear stiffness of the interparticle junctions is correlated to the forces of dry-state particle cohesion.

We thank Maxtek, Inc., Q-Sense, and the Center for Polymer Interfaces and Macromolecular Assemblies, an NSF Materials Research Science and Engineering Center, for funding this research.

*Corresponding author.
Electronic address: curt.frank@stanford.edu
†Corresponding author.
Electronic address: johannsmann@pc.tu-clausthal.de

[1] L. Bocquet, E. Charlaix, and F. Restagno, C.R. Phys. **3**, 207 (2002).
[2] J. Duran and R. Jullien, Phys. Rev. Lett. **80**, 3547 (1998).
[3] T. C. Halsey and A. J. Levine, Phys. Rev. Lett. **80**, 3141 (1998).
[4] D. J. Hornbaker, R. Albert, I. Albert, A. L. Barabási, and P. Schiffer, Nature (London) **387**, 765 (1997).
[5] L. Bocquet, E. Charlaix, S. Ciliberto, and J. Crassous, Nature (London) **396**, 735 (1998).
[6] D. Geromichalos, M. M. Kohonen, F. Mugele, and S. Herminghaus, Phys. Rev. Lett. **90**, 168702 (2003).
[7] J. Israelachvili, *Intermolecular and Surface Forces* (Academic Press, San Diego, 1992).
[8] S. Herminghaus, Adv. Phys. **54**, 221 (2005).
[9] J. M. Valverde, A. Castellanos, A. Ramos, and P. K. Watson, Phys. Rev. E **62**, 6851 (2000).
[10] J. Gao, W. D. Luedtke, D. Gourdon, M. Ruths, J. Israelachvili, and U. Landman, J. Phys. Chem. B **108**, 3410 (2004).
[11] E. Riedo, F. Lévy, and H. Brune, Phys. Rev. Lett. **88**, 185505 (2002).
[12] N. Fraysse, H. Thomé, and L. Petit, Eur. Phys. J. B **11**, 615 (1999).
[13] F. Restagno, C. Ursini, H. Gayvallet, and E. Charlaix, Phys. Rev. E **66**, 021304 (2002).
[14] G. L. Dybwad, J. Appl. Phys. **58**, 2789 (1985).
[15] P. Berthoud and T. Baumberger, Proc. R. Soc. A **454**, 1615 (1998).
[16] M. Kappl and H. J. Butt, Part. Part. Syst. Charact. **19**, 129 (2002).
[17] D. Johannsmann, K. Mathauer, G. Wegner, and W. Knoll, Phys. Rev. B **46**, 7808 (1992).
[18] D. Johannsmann, Macromol. Chem. Phys. **200**, 501 (1999).
[19] S. Berg, D. Johannsmann, and M. Ruths, J. Appl. Phys. **92**, 6905 (2002).
[20] S. Berg and D. Johannsmann, Phys. Rev. Lett. **91**, 145505 (2003).
[21] B. Borovsky, J. Krim, S. Syed Asif, and K. Wahl, J. Appl. Phys. **90**, 6391 (2001).
[22] A. Laschitsch and D. Johannsmann, J. Appl. Phys. **85**, 3759 (1999).
[23] K. K. Kanazawa, Faraday Discuss. **107**, 77 (1997).
[24] W. B. Haines, J. Agric. Sci. **15**, 529 (1925).
[25] H. M. Princen, J. Colloid Interface Sci. **26**, 249 (1968).